JOURNAL OF SOLID STATE CHEMISTRY 20, 417–422 (1977)

Electron Microscopy of the Perovskite-Related Phases 4*H* $Ba_{0.1}Sr_{0.9}MnO_{2.96}$, 5*H* $Ba_5Nb_4O_{15}$ and 6*H* $BaFeO_{2.79}$

J. L. HUTCHISON

Edward Davies Chemical Laboratories, Aberystwyth SY21 1NE, Wales

AND A. J. JACOBSON*

Inorganic Chemistry Laboratories, South Parks Road, Oxford OX1 3QR, England

Received October 15, 1976; in final form December 13, 1976

Lattice images of 4*H*, 5*H*, and 6*H* perovskite polytypes have been obtained. With the electron beam parallel to ⟨10$\bar{1}$0⟩, the images are correlated directly with the projected structures of the polytypes. Stacking faults were found only in the 6*H* compound, and consisted of additional cubic close-packed AO_3 layers. Ordering of cation vacancies in the 5*H* material was evident in the lattice image as an array of white dots.

Introduction

Lattice imaging is now accepted as one of the most useful techniques for the investigation of real crystals. Most high-resolution studies in oxide chemistry have so far been restricted to "open" network structures based on the ReO_3 structure type, and only a few studies have been carried out in more closely packed systems.

Perovskite related phases of general formula ABO_{3-x} can be described in terms of cubic (c) or hexagonal (h) stacking of AO_3 layers with *B* cations in octahedral holes surrounded by oxygens only (*1*). If the layers are cubic close packed, the BO_6 octahedra are all corner-sharing to give the ideal cubic structure as found, for example, in $BaZrO_3$. Deviations from cubic stacking may be partly understood in terms of the tolerance factor (*2*) defined as $t = r_A + r_O/2^{1/2}(r_B + r_O)$ which, for perfect close packing, is equal to 1. When $t > 1.0$ structures with mixed cubic and hexagonal or pure hexagonal stacking are formed. In the hexagonal stacked system the octahedra all share faces and form isolated chains parallel to the *c* axis. Relatively large *A* cations can be accommodated in this structure by adjustment of the *c*/*a* ratio since the chains are not cross linked. In the intermediate range, $1.0 < t < 1.05$–1.06, three mixed stacked sequences are commonly found and are exemplified by 6*H* $BaTiO_3$, 4*H* $SrMnO_3$ and 9*R* $BaRuO_3$[1] However, several factors other than size may operate in particular cases and many other structures are found. In particular, the presence of vacant lattice sites, either anion or cation, has a direct influence on the stacking sequences adopted by the phases examined in this work.

The introduction of hexagonal stacking into a system containing highly charged *B* cations results in a considerable loss in Madelung energy as a consequence of cation repulsions between face-shared octahedra. However, when the system also contains a *B* cation vacancy or a low charged *B* cation, the hexagonal stacking may be stabilized by cation ordering. Thus $Ba_5Ta_4O_{15}$ (*3*) and $Ba_4Ta_3LiO_{12}$

* Present address: Exxon Research and Engineering Co., P.O. Box 45, Linden, N.J. 07036.

[1] *H* and *R* refer to hexagonal and rhombohedral symmetry, respectively; the prefixed number is the number of AO_3 layers in the unit well.

ISSN 0022-4596

TABLE I

Polytype	Compound	a (Å)	c (Å)	Space group	Reference
$4H$	$Ba_{0.1}Sr_{0.9}MnO_{2.96}$	5.466	9.095	$P6_3/mmc$	7
$5H$	$Ba_5Nb_4O_{15}$	5.78	11.72	$P\bar{3}ml$	3
$6H$	$BaFeO_{2.79}$	5.68	13.97	$P6_3/mmc$	8

(*4*, *5*) both contain face-shared octahedra occupied by tantalum and either a vacancy or a lithium cation.

For the anion deficient phases $BaMO_{3-x}$ where M is a first-row transition metal, the structure adopted is closely connected with the way in which the oxygen vacancies can be arranged to give the optimum coordination for the two transition metal oxidation states. Thus in the (Ba, Sr)MnO_{3-x} system the change in structure from $4H$ to $6H$ to $10H$ as a function of vacancy content can be partly understood in terms of a preference for the Mn^{3+} ion to adopt trigonal bipyramidal coordination (*6*, *7*). $BaFeO_{3-x}$ has a markedly different phase diagram as a consequence of a preference for tetrahedral Fe^{3+} coordination (*8*, *9*).

In a previous study $8H$ $Ba_4Ta_3LiO_{12}$ and $10H$ $Ba_5W_3Li_2O_{15}$ which had been prepared and characterized by diffraction methods, were used to demonstrate that images from correctly orientated thin crystals could be directly correlated with their structures and in particular with the stacking of the BaO_3 layers (*10*). The technique was extended by the present authors to include the direct derivation of an unknown 12-layer sequence $BaCoO_{2.6}$, which was used as a basis for refinement of neutron powder diffraction data (*11*).

We present here results obtained for three different sequences; $4H$ $Ba_{0.1}Sr_{0.9}MnO_{2.96}$, $6H$ $BaFeO_{2.79}$, and $5H$ $Ba_5Nb_4O_{15}$. The $4H$ and $6H$ compounds were available from a parallel study of their structures and O vacancy distributions (*7*, *8*). The $5H$ compound was included because of the presence of ordered B cation vacancies as there has been much recent speculation about the criteria for the detection of vacancies in lattice images (*12*).

Structural data for the three systems are presented in Table I. The structures of $4H$ $Ba_{0.1}Sr_{0.9}MnO_{2.96}$ $(ch)_2$ and $6H$ $BaFeO_{2.79}$ $(cch)_2$ are shown in Figs. 1 and 2. The $4H$-structure may be described as pairs of face-shared MnO_6 octahedra sharing corners, and the $6H$ as face-shared pairs of FeO_6 octahedra corner linked to single FeO_6 octahedra. The $5H$ $Ba_5Nb_4O_{15}$ (ccchh) structure is shown in Fig. 3 and consists of a string of three face-sharing NbO_6 octahedra (central one empty) corner linked to a further pair of corner-linked octahedra.

Experimental

Details of sample preparation for the $4H$ and $6H$ compounds were described elsewhere. The $5H$ niobate was prepared by twice firing $BaCO_3$ and Nb_2O_5 (Johnson Matthey "Spec-Pure") at 1350°C for 48 hr. Crushed samples

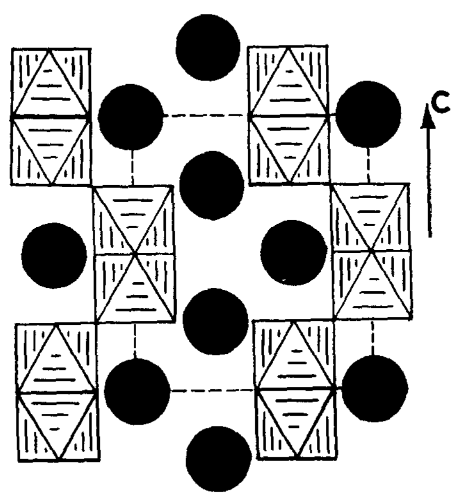

FIG. 1. Idealized $4H$ $Ba_{0.1}Sr_{0.9}MnO_{2.96}$ structure, showing octahedron linkages; boxes show the $[MnO_6]$ octahedra; closed circles show barium atoms.

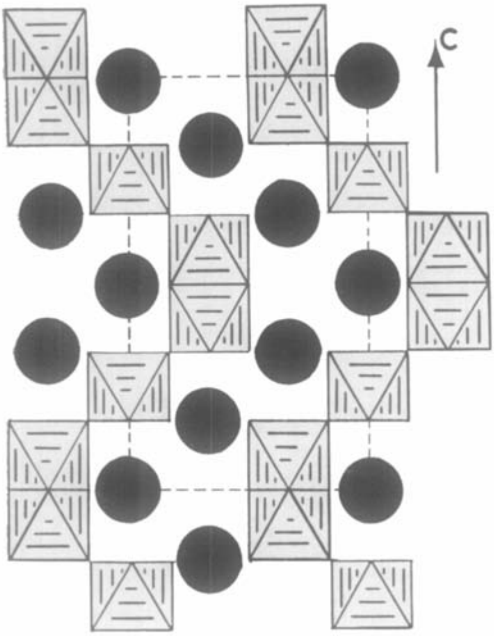

FIG. 2. Idealized $6H$ $BaFeO_{2.79}$ structure.

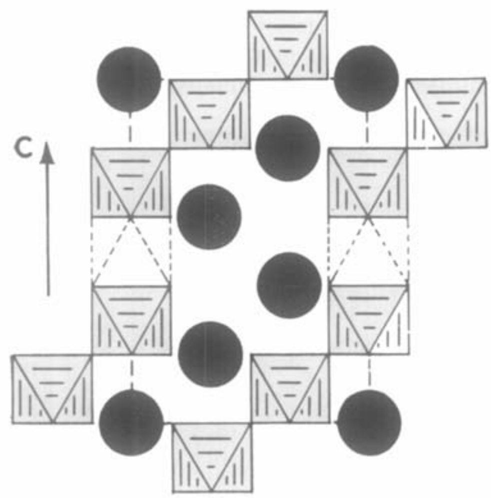

FIG. 3. Idealized $5H$ $Ba_5Nb_4O_{15}$ structure; boxes show the $[NbO_6]$ octahedra; dashed lined boxes show the B-cation vacancies; closed circles show barium atoms.

were mounted on perforated carbon films and examined in a Siemens Elmiskop 102 electron microscope with an accelerating voltage of 100 kV. Suitably thin crystals were sought which could be oriented, using a $\pm 45°$ double stilt stage, so that the electron beam was incident along $\langle 10\bar{1}0 \rangle$. Images were recorded at magnifications of 500,000 using a 40-μm aperture to include all diffracted beams out to 3 nm^{-1}. Images were recorded at a slight underfocus of the objective lens, the condition at which a one-to-one correspondence between image contrast and the projected charge density obtains.

Interpretation of Lattice Images

Lattice images obtained under the above conditions are shown in Figs. 4, 5, and 6. The images of $Ba_{0.1}Sr_{0.9}MnO_{2.96}$ ($4H$) and $BaFeO_{2.79}$ ($6H$) are both similar in that they display an array of alternating black and grey chevrons. The former correspond to rows of barium (or barium–strontium) atoms projected end on, alternating with rows of corner and face-sharing BO_6 octahedra. The separation between dark chevrons is about 5.6 Å, in good agreement with the lattice parameters. The reversal in slope in these chevrons indicates a hexagonal close-packed arrangement of the associated oxygens and allows one to determine the stacking sequence directly from the image.

Results

In the $4H$ material, slope reversals were found every 4.8 Å (every two layers), corresponding to the stacking sequence $(ch)_2$. No faults were observed in this material.

In the $6H$ $BaFeO_{2.79}$ the mirror planes occurred on every third layer, confirming a stacking sequence of $(cch)_2$. A single, isolated stacking fault was found as a missing mirror plane. This corresponds to the *replacement* of a single hexagonal layer by a cubic one, giving a sequence –cchccccchcch–; it could also be regarded as the *insertion* of three extra cubic layers –cchcc*ccc*hcch–. Insertion of extra cubic layers would reflect some compositional inhomogeneity in that $6H$ $BaFeO_{3-x}$ exists in the range $0.05 \geqslant x \geqslant 0.27$, whereas below $x = 0.27$ there exists a two-phase region between $6H$ $BaFeO_{2.63}$ and brownmillerite, $BaFeO_{2.5}$ with all cubic stacking. As oxygen does not contribute significantly to the image

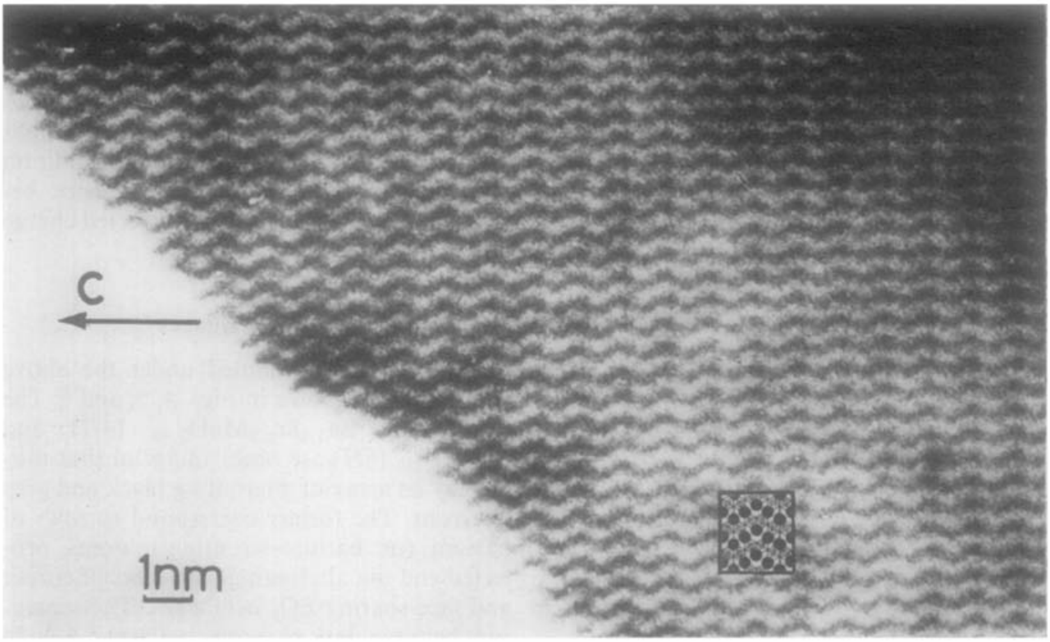

FIG. 4. ⟨10$\bar{1}$0⟩ lattice image of $Ba_{0.1}Sr_{0.9}MnO_{2.96}$, with idealized projection inset; shaded parallelograms show the $[MnO_6]$ octahedra; closed circles show barium atoms.

contrast, the image was not affected by the oxygen vacancies, even although their distribution had been shown to be nonrandom (*8*).

The lattice images of 10*H* $Ba_5W_3Li_2O_{15}$ described earlier (*10*) contained prominent white contrast which was correlated with positions

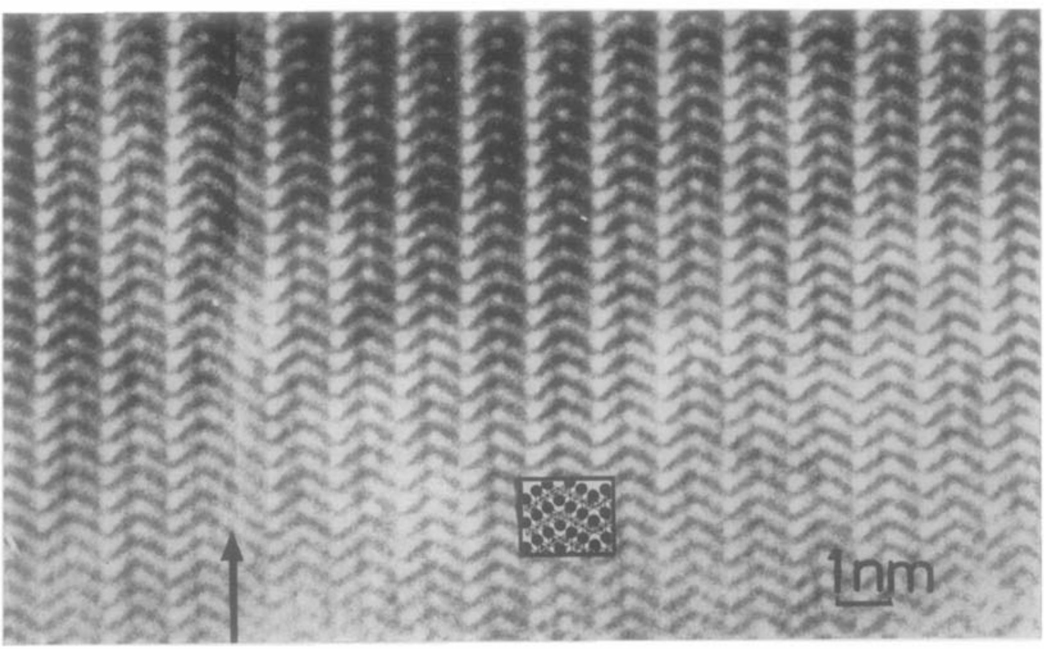

FIG. 5. ⟨10$\bar{1}$0⟩ lattice image of $BaFeO_{2.79}$, with idealized projection inset.

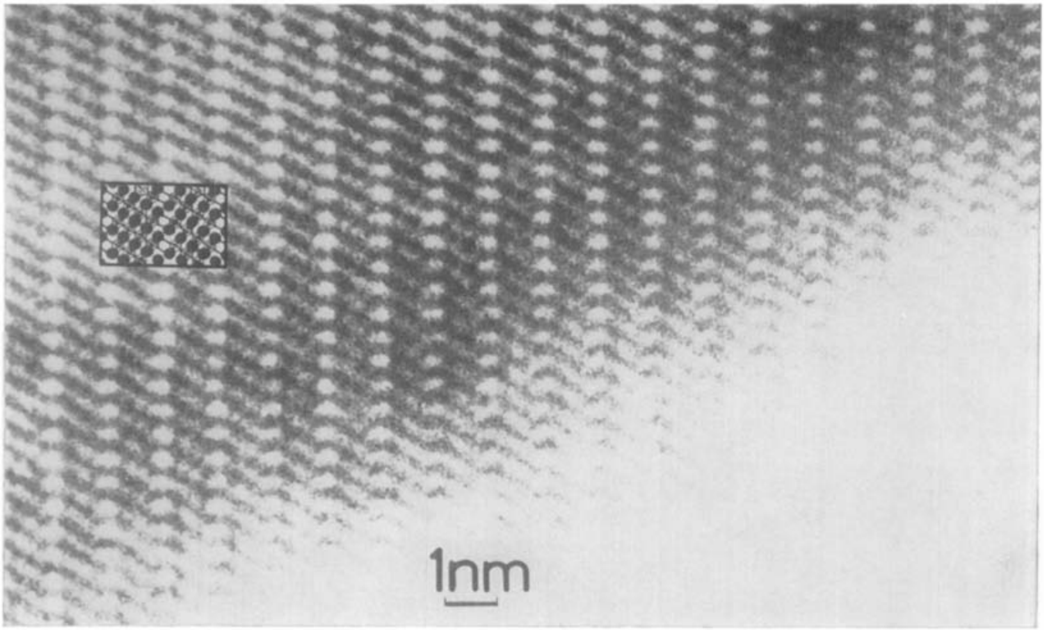

FIG. 6. ⟨10$\bar{1}$0⟩ lattice image of $Ba_5Nb_4O_{15}$ with idealized projection inset; open parallelograms show *B*-cation vacancies.

of ordered arrays of weakly scattering lithiums. In the image of 5*H* $Ba_5Nb_4O_{15}$, the geometry of the dark chevrons confirms the stacking sequence as (ccchh), while the *B*-positions bounded by two h-layers (the central of three face-sharing octahedra) show up as prominent white dots. These positions correspond to projected rows of *B*-site vacancies, as shown inset in Fig. 6. This is in agreement with the published X-ray structure (*3*) and demonstrates for the first time, interpretable lattice image contrast arising from cation vacancies.

Conclusion

With this paper we conclude our experimental survey of the multilayer hexagonal perovskite polytypes, having dealt with 4*H*, 5*H*, and 6*H* (this paper), 8*H* and 10*H* (*10*) and 12*H* (*11*). We have demonstrated that a completely unambiguous interpretation of images is possible with correctly oriented thin crystals. Although the oxygen atoms themselves do not give appreciable contrast, they define the positions of the *A*-site cations which in turn are identified as the dark contrast in the images. Single stacking faults were observed in the 6*H* material, whereas neither the 4*H* nor the 5*H* showed any stacking disorder. Ordering of cation vacancies was confirmed in the 5*H* sample. Further studies of these systems will include a comparison of the experimental results with lattice image calculations.

Acknowledgements

The authors thank the Science Research Council for its support of this work, and J. S. Anderson, F.R.S. for his helpful comments.

References

1. L. KATZ AND R. WARD, Inorg. Chem. **3**, 205, (1964).

2. J. B. GOODENOUGH AND J. M. LONGO, "Crystallographic and Magnetic Properties of Perovskite and Perovskite Related Compounds," Landolt-Bornstein, New Series, Group III/Vol. 4a, Springer-Verlag, New York (1970).

3. J. SHANNON AND L. KATZ, *Acta Cryst.* **B26**, 102 (1970).

4. T. NEGAS, R. S. ROTH, H. S. PARKER, AND W. S. BROWER, *J. Solid State Chem.* **8**, 1 (1973).
5. B. M. COLLINS, A. J. JACOBSON, AND B. E. F. FENDER, *J. Solid State Chem.* **10**, 29 (1974).
6. T. NEGAS, *J. Solid State Chem.* **6**, 136 (1973).
7. A. J. JACOBSON AND A. J. W. HORROX, *Acta Cryst.* **B32**, 1003 (1976).
8. A. J. JACOBSON, *Acta Cryst.* **B32**, 1087 (1976).
9. T. NEGAS AND R. S. ROTH, *J. Res. Nat. Bur. Standards* **73A**, 425 (1969).
10. J. L. HUTCHISON AND A. J. JACOBSON, *Acta Cryst.* **B31**, 1442 (1975).
11. A. J. JACOBSON AND J. L. HUTCHISON, *J. Chem. Soc. Chem. Comm.* 116 (1976).
12. Y. NAKAJIMA, N. MORIMOTO, AND E. WATANABE, *Proc. Japan Acad.* **51**, 173 (1975).